Optimal Test Point Placement Based on Fault Diagnosability Quantitative Evaluation

XIAN-JUN SHI, YU-FENG QIN[iD], AND LI ZHAO
College of Coastal Defense Force, Naval Aviation University, Yantai 264001, China

Corresponding author: Yu-Feng Qin (hy_qyf082@163.com)

ABSTRACT The optimal test point placement problem in existing research results is mainly limited to the qualitative study of whether faults can be diagnosed without considering the difficulty of diagnosing faults. We proposed an optimal test point placement approach based on fault diagnosability quantitative evaluation to solve the above problem. First, the fault diagnosability is quantitatively evaluated based on the maximum mean discrepancy (MMD). Then, the problem of optimal test point placement is considered a multi objective optimization problem. The optimal test point set is solved using the multi objective sparrow search algorithm (MOSSA) based on the fault diagnosability quantitative evaluation results, considering limitations on the test point number, reliability, and cost. Finally, the proposed approach is used to optimize the placement of test points in the switching power supply system. The simulation results show that only three test points need to be placed to make the system meet the fault diagnosability requirements. Two test point placement schemes are obtained, which can be selected according to different practical requirements. The experimental results illustrate that the proposed approach can optimize the system test point placement while ensuring good fault diagnosability.

I. INTRODUCTION

As systems become more complex in function and composition, the probability of failure increases. Fault diagnosis techniques are the key to ensuring the safe, correct, and efficient operation of the system. Scholars have conducted extensive research on fault diagnosis techniques [1]–[3]. However, fault diagnosis cannot be performed if the measurement data does not reflect the fault information adequately. Therefore, it is necessary to improve the fault diagnosability and fundamentally improve the fault diagnosis capability of the system.

Fault diagnosability is the basis of fault diagnosis, including fault detectability and fault isolability [4]. As an essential design characteristic, fault diagnosability fundamentally reflects the ability of the system to diagnose faults. Fault diagnosability research mainly includes fault diagnosability evaluation and fault diagnosability design [5], [6]. Fault diagnosability evaluation measures the ability to detect and isolate faults, which can obtain the difficulty of diagnosing faults in the system under the current resource allocation.

The associate editor coordinating the review of this manuscript and approving it for publication was Mehrdad Saif[iD].

For faults with low diagnosability or can not be diagnosed, improving the fault diagnosis algorithm alone cannot effectively improve the fault diagnosis effect. Then the test points in the system need to be optimally placed to obtain more fault information or enhance the quality of the obtained fault information. Thus, fault diagnosability evaluation can guide optimal test point placement. The results of fault diagnosability evaluation can be qualitative [7], [8] or quantitative [9]–[12]: qualitative evaluation indicates whether faults can be detected or isolated, and quantitative evaluation measures the difficulty of detecting or isolating faults. When the fault diagnosability index is low, the system needs to be optimally designed. In general, fault diagnosability can be enhanced by adding test points or sensors to increase the measurement information [13]. However, the system structure and economic conditions limit the location and number of test points. Moreover, adding test points can reduce overall reliability. Therefore, the problem of optimal test point placement to improve system fault diagnosability needs to be further investigated.

The optimal test point placement meets the fault diagnosis requirements most economically and reliably by

optimizing the number and location of test points or other parameters. Ye *et al.* proposed a test optimization selection method based on the improved binary particle swarm algorithm for the problem that critical faults with a small probability of occurrence are easily missed [14]. Sun *et al.* considered the uncertainty in the test and diagnostic process and proposed an optimal test point selection method under test unreliability conditions [15]. Han *et al.* based on NSGA-3 multi objective optimization algorithm and Bayesian networks to selection test scheme [16]. Saeedi *et al.* constructed a fault isolation table to obtain the minimum test set that can diagnose all faults by continuously selecting the tests associated with the maximum fault numbers [17]. Zhai *et al.* proposed a multi objective test optimization selection method based on NSGA-II under unreliable testing conditions [18]. Yassine *et al.* proposed an approach based on the structural model and Dulmage-Mendelsohn decomposition for optimal sensor placement. The approach assumes that the setup cost of the sensor is defined for each possible variable, and the minimum cost sensor configuration solution is found according to the diagnosability criterion [19]. Liu *et al.* defined fault detectability and isolability criteria based on fault propagation directed graphs and then designed a minimum cost sensor configuration method [20]. Song *et al.* combined the symbolic directed graph model with fuzzy probability and proposed an optimal design method for sensor distribution based on fault propagation weights and monitoring costs [21]. However, the existing results focus on qualitative studies, i.e., each test point to fault diagnosability is focused on the qualitative evaluation of whether the fault can be diagnosed without considering the influence of test points placement on the ease of fault diagnosis.

As a kernel learning method, maximum mean discrepancy (MMD) was first proposed to solve the two-sample detection problem, determining whether two distributions are identical. Nowadays, MMD has been widely used in machine learning and statistics. For example, Long *et al.* incorporated MMD into deep neural networks to construct an adaptive normalized subspace migration learning framework [22]. Based on MMD, Jia *et al.* proposed a new anomaly detector to evaluate the applicability of the studied data or the extracted feature set for fault prediction and health management tasks [23]. Li *et al.* proposed a deep migration learning method based on MMD to solve the problem of rolling bearing fault diagnosis using unlabeled data [24]. Han *et al.* proposed a novel migration learning method based on hybrid distance-guided adversarial networks using Wasserstein distance and MMD for measuring domain distances in different metric spaces to improve domain alignment [25]. Wang *et al.* introduced a loss function based on MMD in deep transfer networks to extract similar latent features and reduce the distribution differences between source and target data [26]. In measuring the difference between the distributions, MMD has the advantage over Kullback-Leibler divergence [27] and Barotropic coefficient [28]. MMD is a measure of distance, satisfying positive definiteness, symmetry, and triangular

inequality; MMD can also reflect the difference between distributions even if the two distributions do not overlap or overlap very little.

This paper proposes an optimal test point placement approach based on fault diagnosability quantitative evaluation to address the shortcomings of the current results. First, fault diagnosability is quantitatively evaluated based on MMD. Then, the multi objective sparrow search algorithm is used to calculate test point sets that meet the fault diagnosability requirements. Thus, fault diagnosability is incorporated as a system feature at the beginning of the design process, and a fundamental improvement in fault diagnosability is achieved.

The rest of this paper is organized as follows. Section II introduces the fault diagnosability quantitative evaluation method based on MMD. Section III presents a brief description of the sparrow search algorithm and gives the process to achieve multi objective optimal test point placement based on multi objective sparrow search algorithm (MOSSA). Section IV uses a switching power supply system as an example to verify the proposed method. Finally, Section V gives some conclusions.

II. FAULT DIAGNOSABILITY QUANTITATIVE EVALUATION BASED ON MMD

A. BASIC IDEA

The measurement data obtained when different faults occur in the system may differ. So the fault diagnosability can be judged according to the similarity of measurement data in different fault modes. If there is little similarity between the measurement data when fault f_i occurs and the normal state, f_i is easier to detect. If there is little similarity between the measurement data when fault f_i occurs and fault f_j occurs, f_i and f_j are easier to isolate.

Suppose $X = [x_1, \cdots, x_{n_1}]$, $Y = [y_1, \cdots, y_{n_2}]$ are two random variables, $x_1, \cdots, x_{n_1}$ and $y_1, \cdots, y_{n_2}$ are independent samples of identically distributed random variables and satisfy $X \sim P$, $Y \sim Q$. P and Q are unknown multivariate distributions. MMD measures the similarity between P and Q by calculating any order moments of X and Y. P and Q are identical if any order moments of X and Y are the same. Otherwise, the moment with the largest discrepancy is used to measure the similarity between X and Y. Based on the above analysis, fault diagnosability quantitative evaluation can be converted into the problem of measuring the similarity of measurement data under different fault modes based on the MMD. The specific method is described below.

B. SPECIFIC METHOD

Suppose there are d test points in the system. Since any of these test points can be used, a total of $2^d - 1$ test point combinations can be used for fault diagnosis. The set of all possible test point combinations is denoted as $T = \{T_1, T_2, \cdots T_{2^d-1}\}$, where T_i denotes the ith test point combination, $1 \leq i \leq 2^d - 1$. The normal state is denoted as f_0. Under the λth test point combination T_λ, the measurement

data when fault f_i occurs is denoted as $X_\lambda = \left[x_1^\lambda, \cdots, x_{n_1}^\lambda\right] \in \mathbb{R}^{n_\lambda \times n_1}$; the measurement data when fault f_j occurs is denoted as $Y_\lambda = \left[y_1^\lambda, \cdots, y_{n_2}^\lambda\right] \in \mathbb{R}^{n_\lambda \times n_2}$, where n_λ is the number of test points in the test point combination T_λ.

$\mathcal{H}$ is denoted as a divisible Hilbert space with the inner product $\langle \cdot, \cdot \rangle_\mathcal{H}$ and associated norm $\|\cdot\|_\mathcal{H}$ (The norm on $\mathcal{H}$ is defined as $\|h\|_\mathcal{H} = \langle h, h \rangle^{1/2}$). Suppose $X_\lambda \sim P_\lambda$ and $Y_\lambda \sim Q_\lambda$, then the distances of distributions P_λ and Q_λ on $\mathcal{H}$ can be expressed as [29]:

$$\Delta\left(P_\lambda, Q_\lambda\right) = \sup_{f \in \mathcal{F}} \left|\mathbb{E}_{X_\lambda \sim P_\lambda} f\left(X_\lambda\right) - \mathbb{E}_{Y_\lambda \sim Q_\lambda} f\left(Y_\lambda\right)\right|.$$

$$(1)$$

where $\mathcal{F}$ is a class of real-valued functions on $\mathcal{H}$, $\mathbb{E}$ is the expectation. $\Delta\left(P_\lambda, Q_\lambda\right)$ is called the MMD between P_λ and Q_λ. For the ease of description, we denote $\Delta\left(X_\lambda, Y_\lambda\right) \iff \Delta\left(P_\lambda, Q_\lambda\right)$. (1) defines a pseudo-distance metric between two probability distributions. For $\forall P, Q, R$, a pseudo-distance metric $\Delta\left(\cdot, \cdot\right)$ should satisfy the following conditions [30]:

1) $\Delta\left(P, P\right) = 0$.
2) $\Delta\left(P, Q\right) = \Delta\left(Q, P\right)$.
3) $\Delta\left(P, R\right) \leq \Delta\left(P, Q\right) + \Delta\left(Q, R\right)$.

The choice of $\mathcal{F}$ needs to satisfy two requirements.
1) Equation (1) must be able to measure the distance between distributions, i.e., $\Delta\left(P_\lambda, Q_\lambda\right)$ needs to satisfy:

$$\Delta\left(P_\lambda, Q_\lambda\right) = 0 \Leftrightarrow P_\lambda = Q_\lambda.$$

$$(2)$$

2) $\mathcal{F}$ should be a subset of $\mathcal{H}$ such that $\Delta\left(P_\lambda, Q_\lambda\right)$ is finite.

The following definitions are made to select suitable $\mathcal{F}$ to satisfy the above two requirements.

Definition 1 (Reproducing Kernel Hilbert Space, RKHS): Suppose k is a positive definite kernel, then for $\forall x_1, \cdots, x_n \in \mathcal{H}, \forall \alpha_1, \cdots, \alpha_n$, we can obtain:

$$\sum_{i,j=1}^{n} \alpha_i \alpha_j k\left(x_i, x_j\right) \geq 0.$$

$$(3)$$

The equality sign holds if and only if $\alpha_1 = \cdots = \alpha_n = 0$. Let $\mathcal{X}$ be a nonempty data set, $\phi\left(x\right) = k\left(x, \cdot\right)$. Then there exists a unique real valued functions Hilbert space $H\left(k\right)$ in $\mathcal{H}$ which satisfies:

1) $\forall x \in \mathcal{H}, \phi\left(x\right) \in H\left(k\right)$.
2) $\forall f \in \mathcal{H}, \forall x \in \mathcal{X}, \langle f, \phi\left(x\right) \rangle_{H(k)} = f\left(x\right)$.

$H\left(k\right)$ is called the RKHS of k.

Definition 2 (Characteristic Kernel): $\mathcal{B}\left(k\right) = \{f \in H\left(k\right) | \|f\|_{H(k)} \leq 1\}$ is denoted as the unit ball on $H\left(k\right)$. Assume that $\mathcal{F}$ and k satisfy $\mathcal{F} = \mathcal{B}\left(k\right)$. If $\Delta\left(P, Q\right) = 0 \Leftrightarrow P = Q$, then k is called the characteristic kernel. Common characteristic kernels include the Gaussian kernel $k\left(x, y\right) = \exp\left(-\frac{\|x-y\|^2}{2\sigma^2}\right)$, Exponential kernel $k\left(x, y\right) = \exp\left(-\frac{\|x-y\|}{2\sigma^2}\right)$, Laplacian kernel $k\left(x, y\right) = \exp\left(-\frac{\|x-y\|}{\sigma}\right)$, $\sigma > 0$, etc.

Definition 3: (Kernel Mean Embedding) Suppose P satisfies $\mathbb{E}_{X \sim P}\left(\sqrt{k\left(X, X\right)}\right) < \infty$. Then there exists
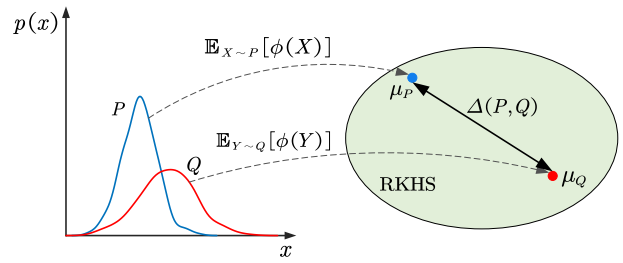
FIGURE 1. The kernel mean embedding framework.

$\mu_P = \mathbb{E}_{X \sim P}\left[\phi\left(X\right)\right] \in H\left(k\right)$ such that for $\forall f \in H\left(k\right)$:

$$\begin{aligned}
\mathbb{E}f\left(X\right) &= \int_{\mathcal{X}} p\left(\mathrm{d}X\right) f\left(X\right) \\
&= \int_{\mathcal{X}} p\left(\mathrm{d}X\right) \langle \phi\left(X\right), f \rangle_{H(k)} \\
&= \int_{\mathcal{X}} \langle p\left(\mathrm{d}X\right) \phi\left(X\right), f \rangle_{H(k)} \\
&= \langle \mu_P, f \rangle_{H(k)}.
\end{aligned}$$

$$(4)$$

μ_P is called the kernel mean embedding of P in $H\left(k\right)$.

It can be seen that taking $\mathcal{F} = \mathcal{B}\left(k\right)$ while k is the characteristic kernel can solve the two requirements mentioned before from above definitions. Then (1) can be rewritten as:

$$\begin{aligned}
&\Delta\left(P_\lambda, Q_\lambda\right) \\
&= \sup_{f \in H(k), \|f\|_{H(k)} \leq 1} \left|\mathbb{E}_{X_\lambda \sim P_\lambda} f\left(X_\lambda\right) - \mathbb{E}_{Y_\lambda \sim Q_\lambda} f\left(Y_\lambda\right)\right| \\
&= \sup_{f \in H(k), \|f\|_{H(k)} \leq 1} \left|\langle \mu_{P_\lambda}, f \rangle_{H(k)} - \langle \mu_{Q_\lambda}, f \rangle_{H(k)}\right| \\
&= \sup_{f \in H(k), \|f\|_{H(k)} \leq 1} \left|\langle \mu_{P_\lambda} - \mu_{Q_\lambda}, f \rangle_{H(k)}\right|.
\end{aligned}$$

$$(5)$$

According to the characteristics of the norm, we can get:

$$\begin{aligned}
&\left|\langle \mu_{P_\lambda} - \mu_{Q_\lambda}, f \rangle_{H(k)}\right| \\
&\leq \|\mu_{P_\lambda} - \mu_{Q_\lambda}\|_{H(k)} \|f\|_{H(k)} \\
&\leq \|\mu_{P_\lambda} - \mu_{Q_\lambda}\|_{H(k)}.
\end{aligned}$$

$$(6)$$

At this point, $\Delta\left(P_\lambda, Q_\lambda\right)$ can represent the discrepancy between the kernel mean embedding of P_λ and Q_λ on RKHS:

$$\begin{aligned}
&\Delta\left(P_\lambda, Q_\lambda\right) \\
&= \sup_{f \in H(k), \|f\|_{H(k)} \leq 1} \left|\langle \mu_{P_\lambda} - \mu_{Q_\lambda}, f \rangle_{H(k)}\right| \\
&= \|\mu_{P_\lambda} - \mu_{Q_\lambda}\|_{H(k)}.
\end{aligned}$$

$$(7)$$

Fig. 1 shows the kernel mean embedding framework. The distribution is mapped to a point in RKHS, and the distance between two distributions can be calculated by the inner product.

μ cannot be calculated directly. Since the sample mean is an unbiased estimate of the expectation, the sample mean is used to calculate μ. The value of $\Delta\left(P_\lambda, Q_\lambda\right)$ depends on the

discrepancy between the means of $\phi(X_\lambda)$ and $\phi(Y_\lambda)$ in $H(k)$:

$$
\begin{aligned}
&\Delta(P_\lambda, Q_\lambda)^2 \\
&= \|\mu_{P_\lambda} - \mu_{Q_\lambda}\|^2_{H(k)} \\
&= \|\frac{1}{n_1}\sum_{i=1}^{n_1}\phi(x_i^\lambda) - \frac{1}{n_2}\sum_{j=1}^{n_2}\phi(y_j^\lambda)\|^2_{H(k)} \\
&= \frac{1}{n_1^2}\sum_{i,j=1}^{n_1}\langle\phi(x_i^\lambda),\phi(x_j^\lambda)\rangle + \frac{1}{n_2^2}\sum_{i,j=1}^{n_2}\langle\phi(y_i^\lambda),\phi(y_j^\lambda)\rangle \\
&\quad - \frac{2}{n_1 n_2}\sum_{i,j=1}^{n_1,n_2}\langle\phi(x_i^\lambda),\phi(y_j^\lambda)\rangle.
\end{aligned}
\tag{8}
$$

According to the reproducibility of $H(k)$, we can get:

$$
\begin{aligned}
\langle\phi(x_i^\lambda),\phi(x_j^\lambda)\rangle_{H(k)} &= \langle\phi(x_i^\lambda),k(x_j^\lambda,\cdot)\rangle_{H(k)} \\
&= k(x_i^\lambda,x_j^\lambda).
\end{aligned}
\tag{9}
$$

Thus, (8) can be expressed as:

$$
\begin{aligned}
&\Delta(P_\lambda,Q_\lambda)^2 \\
&= \frac{1}{n_1^2}\sum_{i,j=1}^{n_1}k(x_i^\lambda,x_j^\lambda) + \frac{1}{n_2^2}\sum_{i,j=1}^{n_2}k(y_i^\lambda,y_j^\lambda) \\
&\quad - \frac{2}{n_1 n_2}\sum_{i,j=1}^{n_1,n_2}k(x_i^\lambda,y_j^\lambda).
\end{aligned}
\tag{10}
$$

The fault diagnostic performance is related to the selected test points. Since any test point combination can perform fault diagnosis, the maximum value of MMD of all test point combinations is taken as the fault diagnosability evaluation result. According to the above analysis, the fault diagnosability evaluation formula can be expressed as follows:

$$
D(f_i,f_j) = \max\{\Delta(P_\lambda,Q_\lambda)\}.
\tag{11}
$$

where $i, j = 0, 1, \cdots, i \neq j, \lambda = 1, \cdots, 2^d - 1$. $D(f_i, f_0)$ represents the fault detectability of f_i, $D(f_i, f_j)$ represents the fault isolability between f_i and f_j. The larger of $D(f_i, f_0)$, indicates that f_i has the stronger detectability, and it is easier to be detected. The larger of $D(f_i, f_j)$, indicates that f_i and f_j have the stronger isolability, and they are easier to be isolated. Since a fault does not have isolability from itself, the case of $D(f_i, f_j)$, $i = j$ is not considered. According to (10) and (11), we can get $D(f_i, f_j) = D(f_j, f_i)$.

Detecting f_i can be considered as isolating f_i and f_0. Without considering the measurement noise, if f_i and f_j are not isolable, then $D(f_i, f_j) = 0$. However, due to the inevitable existence of various disturbing factors in the actual measurement process, the fault diagnosability evaluation result will be slightly larger than 0. Therefore, if f_i and f_j are not isolable, then denote $D(f_i, f_j) = \xi$. ξ can be determined by calculating the MMD between the two measurement data sets under same states using all d test points. Then it is necessary to design the diagnosability threshold ε. If $D(f_i, f_0) > \varepsilon, f_i$ is detectable, otherwise f_i can not be detected; if $D(f_i, f_j) > \varepsilon$, f_i and f_j are isolable, otherwise f_i and f_j can not be isolated.

The diagnosability threshold ε affects the diagnosability of faults and should be selected according to the measurement noise intensity. The greater the intensity of the measurement noise, the larger the ε should be.

III. OPTIMAL TEST POINT PLACEMENT
Theoretically, if test points are placed at all possible locations in the system, the fault diagnosability can be maximized. However, the above solution is not feasible in practice. Therefore, it is necessary to optimize the test point placement considering the space, reliability, cost, or other objectives. Therefore, this paper proposes an optimal test point placement approach based on MOSSA to provide a new way for optimal test point placement research.

A. CONSTRAINT FUNCTIONS
Suppose there are m faults. Since the fundamental purpose of optimal test point placement is to ensure that the system has good fault diagnosability, the qualitative evaluation and quantitative evaluation of the fault diagnosis capability are considered in this paper. The following four constraint functions are proposed for the test point placement process.

1) FAULT DIAGNOSABILITY QUANTITATIVE EVALUATION INDEX CONSTRAINTS
a: FAULT DETECTABILITY INDEX (FDI)
If a fault is undetectable, then the fault is not isolable from other faults. It shows that fault detectability is the basis of fault diagnosis. Therefore, the FDI needs to be a constraint. Denote the test point set as $\Omega = \{t_1, \cdots, t_d\}$. The detectability of all faults can be maximized if we place all test points. The overall FDI of the system is denoted as:

$$
\text{FDI} = \sum_{i=1}^{m} D(f_i, f_0)
\tag{12}
$$

In practice, the FDI should be kept in a good range, and not all test points need to be placed. The optimal test point placement should satisfy the following constraint:

$$
\text{FDI} \geq \text{FDI}_{\text{req}}
\tag{13}
$$

where FDI_{req} is the minimum FDI required to be achieved. Under this requirement, the test point set Ω_{req} is a subset of Ω.

b: FAULT ISOLABILITY INDEX (FII)
Fault isolability is the basis for fault isolation. Fault isolation includes not only detecting faults but also isolating between different faults. The isolability between all faults can be maximized if we place all test points in Ω. The overall FII of the system is denoted as:

$$
\text{FII} = \sum_{\substack{i,j=1,2 \\ i \neq j-1}}^{m,m+1} D(f_i, f_j)
\tag{14}
$$

Similar to the fault detectability index constraint, the FII should satisfy the following constraint:

$$\text{FII} \geq \text{FII}_{\text{req}} \tag{15}$$

where FII_{req} is the minimum level of fault isolability index required to be achieved.

Although the fault diagnosability quantitative evaluation is the main factor to be considered, it also needs to consider the qualitative evaluation result. The aim is to avoid some faults having a high diagnosability index while others can not be diagnosed. Thus, we also design fault detection rate (FDR) and fault isolation rate (FIR) constraints.

2) FAULT DIAGNOSABILITY QUALITATIVE EVALUATION INDEX CONSTRAINTS

a: FDR
The fault detection rate is the ratio of all detectable faults to the total number of faults. The equation is shown as follows:

$$\text{FDR} = \frac{m_D}{m} \times 100\% \tag{16}$$

where m_D is the total number of detectable faults, m is the total number of faults. The system FDR should satisfy the following constraint:

$$\text{FDR} \geq \text{FDR}_{\text{req}} \tag{17}$$

where FDR_{req} is the minimum level of fault detection rate that the system is required to achieve.

b: FIR
The fault isolation rate is the ratio of the total number of individually isolable faults to the total number of all detectable faults. The equation is shown as follows:

$$\text{FDR} = \frac{m_I}{m_D} \times 100\% \tag{18}$$

where m_I is the number of faults that can be individually isolated. The system FIR should satisfy the following constraint:

$$\text{FIR} \geq \text{FIR}_{\text{req}} \tag{19}$$

where FIR_{req} is the minimum level of fault isolation rate that the system is required to achieve.

B. OBJECTIVE FUNCTIONS
We design the following three objective functions in the optimization process.

1) THE NUMBER OF TEST POINTS
Under the test point set $\bar{\Omega}$, the number of test points $n_{\bar{\Omega}}$ is defined as the number of elements in $\bar{\Omega}$.

2) THE RELIABILITY INDEX
Increasing the number of test points in the system could decrease the overall system reliability. Under the test point set $\bar{\Omega}$, the reliability index is defined as:

$$R_{\bar{\Omega}} = \sum_{t_i \in \bar{\Omega}} r_{t_i} \tag{20}$$

where r_{t_i} is the reliability factor of the ith test point t_i in $\bar{\Omega}$, and a smaller value of $R_{\bar{\Omega}}$ indicates a higher overall system reliability.

3) THE COST INDEX
The cost index is mainly composed of the price of test circuit components, installation cost, and post-maintenance cost. The cost index of test point placement under the test point set $\bar{\Omega}$ is defined as:

$$C_{\bar{\Omega}} = \sum_{c_i \in \bar{\Omega}} c_{t_i} \tag{21}$$

where c_{t_i} is the cost factor of the ith test point t_i in $\bar{\Omega}$. A smaller value of $C_{\bar{\Omega}}$ indicates a lower test point placement cost.

C. MULTI OBJECTIVE OPTIMIZATION MODEL
It can be seen from the above analysis that the optimal test point placement problem is a multi objective optimization problem, which can be described by the following model:

$$\begin{cases} \min n_{\bar{\Omega}} \\ \min R_{\bar{\Omega}} \\ \min C_{\bar{\Omega}} \\ \text{FDI} \geq \text{FDI}_{\text{req}} \\ \text{FII} \geq \text{FII}_{\text{req}} \\ \text{FDR} \geq \text{FDR}_{\text{req}} \\ \text{FIR} \geq \text{FIR}_{\text{req}} \end{cases} \tag{22}$$

Under the condition of satisfying these constraints, the optimal test point set is obtained so that the number and cost of test points are as low as possible and the reliability is as high as possible. For this multi objective optimization model, the MOSSA is used in this paper for optimal test points placement based on fault diagnosability.

D. MULTI OBJECTIVE SPARROW SEARCH ALGORITHM
In the sparrow search algorithm, the sparrow population contains three types of individuals: producers, scroungers, and spectators [31], [32]. The producer is responsible for providing the location and direction of food for the whole population. The scrounger follows the producer in foraging. The spectator is responsible for monitoring the area around the food. During the entire process, the positions of all individuals are constantly updated, and then the best position of the food is obtained.

The position of the sparrow can be represented by the following matrix:

$$X = \begin{bmatrix} x_{1,1} & x_{1,2} & \cdots & x_{1,d} \\ x_{2,1} & x_{2,2} & \cdots & x_{2,d} \\ \vdots & \vdots & \ddots & \vdots \\ x_{n,1} & x_{n,2} & \cdots & x_{n,d} \end{bmatrix} \tag{23}$$

where n is the number of individuals in the population, d denotes the number of dimensions of the variable to be

optimized, i.e., the maximum number of test points to be configured. $x_{i,j}$ denotes the jth dimensional value of the ith individual, taking the value 1 or 0: $x_{i,j} = 1$ means the jth test point is placed, $x_{i,j} = 0$ means the jth test point is not placed. The fitness values of all sparrows can be represented by the following vectors:

$$
F_X = \begin{bmatrix} f\left(\begin{bmatrix} x_{1,1} & x_{1,2} & \cdots & x_{1,d} \end{bmatrix}\right) \\ f\left(\begin{bmatrix} x_{2,1} & x_{2,2} & \cdots & x_{2,d} \end{bmatrix}\right) \\ \vdots \\ f\left(\begin{bmatrix} x_{n,1} & x_{n,2} & \cdots & x_{n,d} \end{bmatrix}\right) \end{bmatrix} \tag{24}
$$

where the value of each row in F_X denotes the fitness value.

In SSA, producers with better fitness values are given priority to obtain food during the search. In each iteration, the position of the producer is updated as follows:

$$
x_{i,j}^{t+1} = \begin{cases} x_{i,j}^t \cdot \exp\left(\dfrac{-i}{\alpha \cdot \text{iter}_{\max}}\right) & R_2 < ST \\ x_{i,j}^t + Q \cdot L & R_2 \geq ST \end{cases} \tag{25}
$$

where t denotes the current number of iterations, $j = 1, \cdots, d$. $\text{iter}_{\max}$ is the maximum number of iterations. $\alpha \in (0, 1]$ is a random number. $R_2 \in [0, 1]$ and $ST \in [0.5, 1]$ denote the alarm value and the safety threshold, respectively. Q is a random number obeying normal distribution. $L \in \mathbb{R}^{1 \times d}$ and all elements in L are 1. If $R_2 < ST$, it means there are no predators around, producers enter a wide search mode. If $R_2 \geq ST$, it means that some sparrows have found the predator and all sparrows need to fly to other safe areas.

Some scroungers monitor the producer, and once they find that producers have found good food, they will immediately leave their current position to compete for the food. If scroungers win, they can get the food from producers immediately. The position of the scrounger is updated as follows:

$$
x_{i,j}^{t+1} = \begin{cases} Q \cdot \exp\left(\dfrac{x_{\text{worst},j}^t - x_{i,j}^t}{i^2}\right) & i > n/2 \\ x_{P,j}^{t+1} + \left| x_{i,j}^t - x_{P,j}^{t+1} \right| \cdot A^+ \cdot L & i \leq n/2 \end{cases} \tag{26}
$$

where $x_{P,j}$ denotes the best position of the explorer in the jth dimension. $x_{\text{worst},j}$ denotes the current global worst position of the sparrow in the jth dimension. All elements in $A \in \mathbb{R}^{1 \times d}$ are randomly assigned to 1 or -1, A^+ is the generalized inverse of A. When $i > n/2$, it means that the ith scrounger is most likely to be hungry and go to other positions to feed. Otherwise, the ith scrounger randomly finds a location near the best location for the producer to forage.

The position of the spectator is updated as follows:

$$
x_{i,j}^{t+1} = \begin{cases} x_{\text{best},j}^t + \beta \left| x_{i,j}^t - x_{\text{best},j}^t \right| & f_i > f_g \\ x_{i,j}^t + \mu \dfrac{\left| x_{i,j}^t - x_{\text{worst},j}^t \right|}{(f_i - f_w) + \delta} & f_i = f_g \end{cases} \tag{27}
$$

where $x_{\text{best},j}$ is the current global best position in the jth dimension. $\beta \in N(0, 1)$ is a step control parameter.

$\mu \in [-1, 1]$ is a random number representing the sparrow moving direction. f_i is the current fitness value of the sparrow. f_g and f_w are the current global best and worst fitness values, respectively. δ is a small constant. For simplicity, when $f_i > f_g$, it means that the sparrow is at the edge of the population and is extremely vulnerable to predators; when $f_i = f_g$, it means that the sparrow in the middle of the population is aware of the danger and needs to approach other sparrows.

The optimal test points placement problem belongs to the optimization problem in discrete space. The sigmoid function is used to map the element in the position vector as a probability on $[0, 1]$. The position vector is converted to binary according to the following formula:

$$
\begin{cases} s\left(x_{i,j}^t\right) = \dfrac{1}{1 + e^{-x_{i,j}^t}} \\ x_{i,j}^t = \begin{cases} 0 & s\left(x_{i,j}^t\right) > \tau \\ 1 & s\left(x_{i,j}^t\right) \leq \tau \end{cases} \end{cases} \tag{28}
$$

where τ is a random number in $[0, 1]$.

The steps of the multi objective sparrow search algorithm are described as follows.

Step1: Initialize the population and parameters.

Step2: Calculate the fitness value of individuals in the population, and sort them from minimum to maximum according to the fitness value to find out the current best and worst individuals and their locations.

Step3: Update the producer position according to (25).

Step4: Update the scrounger position according to (26).

Step5: Update the spectator position according to (27).

Step6: Convert individual positions to binary according to (28).

Step7: Determine whether the individuals in the population meet the constraints in (22). Otherwise, go to Step3.

Step8: Calculate the objective function of all individuals after updating the position, get the non-dominated individuals in the updated population, and update the population fitness and position information.

Step9: Determine whether the number of iterations reaches the maximum. If the maximum number of iterations is reached, output the non-dominated individual set, and the loop ends. Otherwise, go to Step2.

The flow chart of the multi objective sparrow search algorithm is shown in Fig. 2.

IV. EXPERIMENTAL ANALYSIS

The primary function of the switching power supply is to complete the electrical energy conversion and power transfer. As one of the most critical units in the power electronic system, it is widely used in various fields such as military equipment, instrumentation, communication equipment, etc. In this paper, a switching power supply system is used as an example to verify the proposed method. The switching power supply adopts the PWM switching control method to convert 220V AC into a controllable constant current source to supply
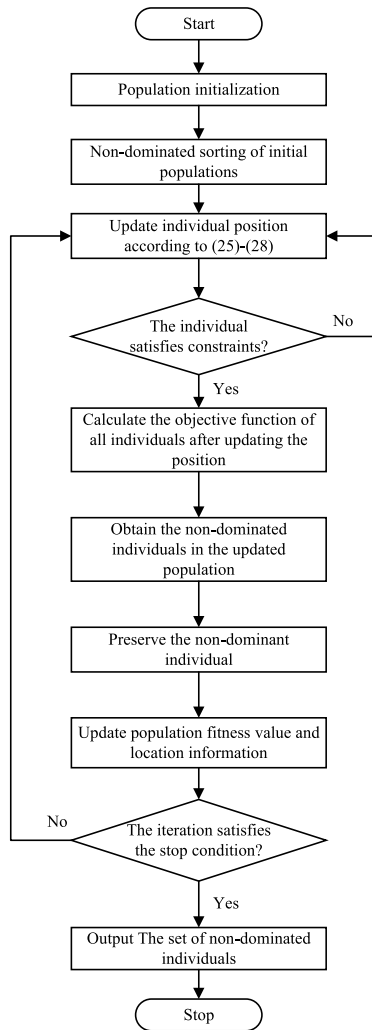
FIGURE 2. Flow chart of the MOSSA.

TABLE 1. Fault mode table.

Fault Number	Faulty component	Fault Type
f_0	—	No-fault
f_1	S	No input signal
f_2	Q_1	Open circuit(D,S)
f_3	U_3	Short circuit(C,E)
f_4	R_{11}	Open circuit
f_5	C_{10}	Short circuit
f_6	R_{15}	Open circuit
f_7	R_6	Open circuit
f_8	R_{18}	Short circuit

the load to realize the conversion of electrical energy. The system schematic and the location of the test points are shown in Fig. 3. The tolerances of all resistors and capacitors are 5% and 10%, respectively, and all test points detect the node voltage signals. The fault modes of some critical components in the system are selected for analysis, as shown in Table. 1, where: Q_1 open circuit fault occurred at the terminals of D, S, U_3 short circuit fault occurred at the terminals of C, E.

TABLE 2. Test points reliability and cost factor.

Test point number	Reliability factor	Cost factor
t_1	0.5	0.2
t_2	0.3	0.35
t_3	0.2	0.35
t_4	0.3	0.8
t_5	0.2	0.8
t_6	0.2	0.8
t_7	0.2	0.8
t_8	0.15	0.45
t_9	0.1	0.5
t_{10}	0.45	0.45
t_{11}	0.35	0.6
t_{12}	0.45	0.6

There are 12 test points in the system, so there are $2^{12} - 1 = 4095$ test point combinations. Our purpose is to select the optimal test point sets that meet the requirements. First, the fault diagnosability under different test point combinations is quantitatively evaluated. Then, the test points are optimally placed based on the fault diagnosability, considering the inherent space limitation of the system and the maintenance cost of these test points. We think that installation and maintenance are more difficult when there are more components and less space near the test point, and therefore the higher the cost factor. At the same time, test points are generally placed in the form of test circuits. Once the test circuit occurs faults, it may increase the failure probability of surrounding components due to electromagnetic interference. Therefore, we make the following assumptions for the reliability factor r_{t_i} and cost factor c_{t_i} of each test point, as shown in Table 2.

A. FAULT DIAGNOSABILITY EVALUATION

Suppose the signal-to-noise ratio of the measured signal is SNR=25dB, the measurement data are collected uniformly from 0 to 5ms. We choose k for the Gaussian kernel and the kernel parameter $\sigma = 1$. For two test datasets under the same condition when all 12 test points are placed, the MMD of both datasets is calculated several times. The noise signal in each calculation is random, and the average value of the MMD is calculated as $\xi = 0.0317$. The result of each calculation does not exceed 0.05. Therefore, take the diagnosability threshold $\varepsilon = 0.05$ to ensure the tolerance. If $D(f_i, f_0) > 0.05$, f_i is detectable; if $D(f_i, f_j) > 0.05$, f_i and f_j are isolable. The quantitative evaluation of fault diagnosability is performed with all 12 test points placed. The result is shown in Table. 3. Where the elements of the ith row and jth column denote $D(f_i, f_{j-1})$, $i = 1, \cdots, 8$, $j = 1, \cdots, 9$. From the fault diagnosability evaluation result, we can know that $D(f_i, f_0) > 0.05$, so all faults are detectable. Where f_3 has the highest detectability: $D(f_3, f_0) = 1.4100$, f_6 has the lowest detectability: $D(f_6, f_0) = 0.9708$. f_3 and f_5 have the highest isolability: $D(f_3, f_5) = 1.4099$, f_5 and f_8 have the lowest isolability: $D(f_5, f_8) = 0.0067$. Since
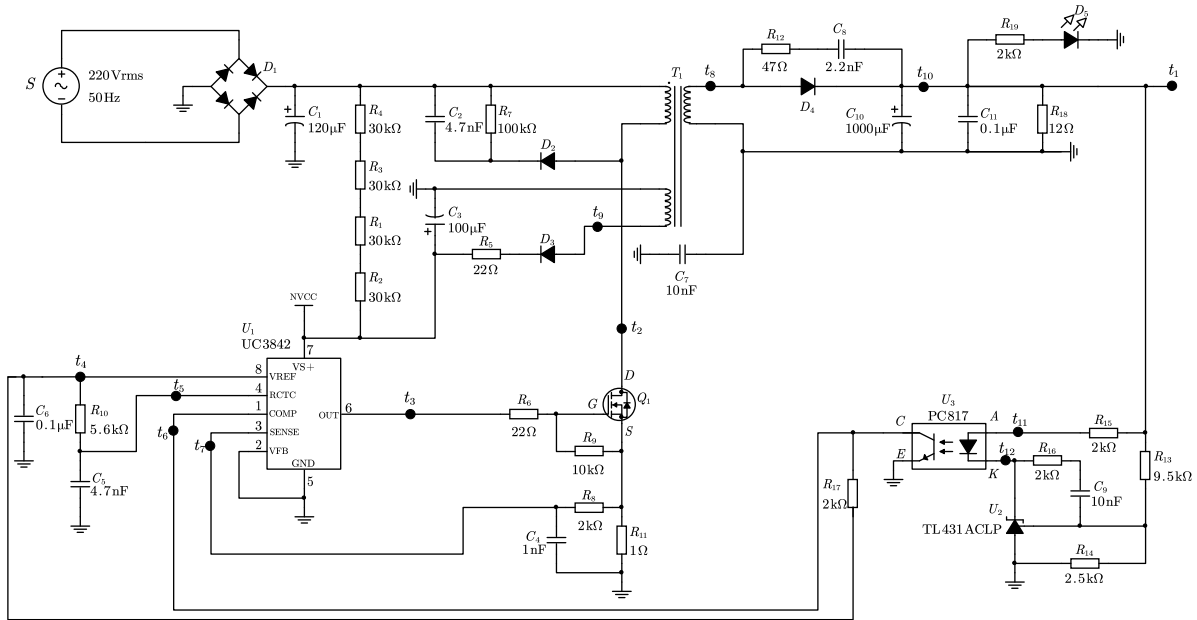
FIGURE 3. Schematic of switching power supply.

$D(f_5, f_8) = 0.0067$, f_5 and f_8 are not isolable. Therefore, it can be obtained that $\text{FDI}_{\max} = \sum_{i=1}^{8} D(f_i, f_0) = 8.4072$,

$\text{FII}_{\max} = \sum_{\substack{i,j=1,2 \\ i \neq j-1}}^{8,9} D(f_i, f_j) = 51.7618$, $\text{FDR}_{\max} = 100\%$,

$\text{FIR}_{\max} = 75\%$. The system reliability index is 3.4, and the cost index is 6.7.

To verify the correctness of the fault diagnosability evaluation results, we use the t-SNE algorithm to project the measurement data into a two dimensional space for visualization. The proposed approach is verified according to the clustering degree of the measurement data. Since $D(f_6, f_7) > D(f_7, f_8) > D(f_5, f_8)$, the experiments are conducted with f_6 and f_7, f_7 and f_8, f_5 and f_8 respectively, in which 50 samples of test signals are collected for each faults, and the simulation results are shown in Fig. 4.

Fig. 4 (a), (b), and (c) show the visualization results of measurement data for $f_6 - f_7$, $f_7 - f_8$, and $f_5 - f_8$, respectively. For f_6 and f_7, the measurement data of the same category are distributed in the same region, and the interval between these two categories is large so that f_6 and f_7 can be clearly isolated. For f_7 and f_8, the measurement data of the same category are only partially distributed in the same area, and there is an overlap between the measurement data of these two categories. For f_5 and f_8, the two categories of measurement data are distributed almost in the same area. Thus, it is difficult to isolate f_5 and f_8. The above results are consistent with the results of fault diagnosability evaluation. Therefore, the diagnosability evaluation results based on the proposed approach are correct. In addition, for faults with low diagnosability, the difference in measurement data can be improved by adding test points or changing the location of test points to improve the actual fault diagnosis effect.

To illustrate the advantages of the method in this paper, the results of fault diagnosability evaluation based on the proposed approach are compared with those based on the K-L divergence [27]. The results of the fault diagnosability evaluation based on K-L divergence are shown in Table. 4. It can be seen that the fault isolability results obtained based on K-L divergence methods are asymmetric, i.e., $D(f_i, f_j) \neq D(f_j, f_i)$. For example, the isolability between f_1 and f_2 is $D(f_1, f_2) = 110.0853$, $D(f_2, f_1) = 2.2194$; the isolability between f_1 and f_4 is $D(f_1, f_4) = 6.1600$, $D(f_4, f_1) = 3.3435e4$. Due to the asymmetric nature of the K-L divergence, there exist the case $D(f_1, f_2) > D(f_1, f_4)$ but $D(f_2, f_1) < D(f_4, f_1)$, it is not possible to determine whether isolating f_2 from f_1 is more difficult than isolating f_4 from f_1. MMD satisfies the symmetry condition as a metric distance, so the fault diagnosability evaluation results obtained based on the proposed approach are symmetric and can clearly reflect the difficulty of fault diagnosis.

B. OPTIMAL TEST POINT PLACEMENT

The fault diagnosability evaluation results in Table. 3 are obtained by placing all 12 test points. However, meeting the desired fault diagnosability level does not need place all test points. Without reducing the FDR and FIR, 85% of the maximum value of the fault diagnosability quantitative evaluation index is used as the minimum requirement for test point placement:

$$\begin{cases} \text{FDI}_{\text{req}} = 0.85\text{FDI}_{\max} \\ \text{FII}_{\text{req}} = 0.85\text{FII}_{\max} \\ \text{FDR}_{\text{req}} = \text{FDR}_{\max} \\ \text{FIR}_{\text{req}} = \text{FIR}_{\max} \end{cases}$$

After determining the system constraint function and objective function, the multi objective sparrow search algorithm

TABLE 3. Fault diagnosability evaluation result based on the proposed approach.

	f_0	f_1	f_2	f_3	f_4	f_5	f_6	f_7	f_8
f_1	1.0301	*	0.2341	1.4096	0.8712	0.9984	1.0300	0.9448	1.0002
f_2	1.0301	0.2341	*	1.4073	0.9897	0.9894	1.0301	0.9705	0.9912
f_3	1.4100	1.4096	1.4073	*	1.4096	1.4099	1.4095	1.4080	1.4098
f_4	0.9890	0.8712	0.9897	1.4096	*	0.2822	0.9920	0.5249	0.2847
f_5	0.9890	0.9984	0.9894	1.4099	0.2822	*	0.9919	0.4458	0.0067
f_6	0.9708	1.0300	1.0301	1.4095	0.9920	0.9919	*	1.0012	0.9920
f_7	0.9991	0.9448	0.9705	1.4080	0.5249	0.4458	1.0012	*	0.4462
f_8	0.9891	1.0002	0.9912	1.4098	0.2847	0.0067	0.9920	0.4462	*

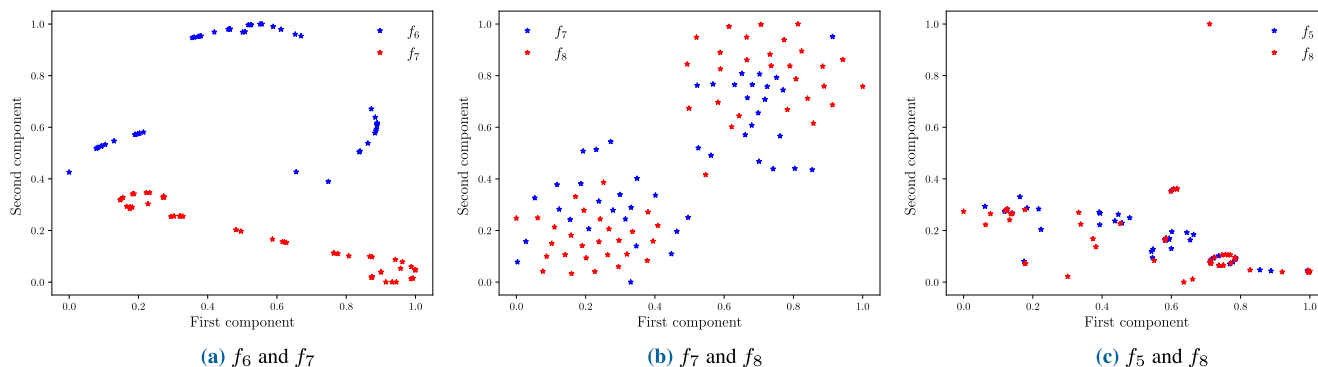**(a)** f_6 and f_7 **(b)** f_7 and f_8 **(c)** f_5 and f_8

FIGURE 4. Data visualization results.

TABLE 4. Fault diagnosability evaluation result based on K-L divergence.

	f_0	f_1	f_2	f_3	f_4	f_5	f_6	f_7	f_8
f_1	$1.6811e4$	*	110.0853	$1.4626e4$	6.1600	9.1302	5.9416	27.3943	9.0887
f_2	$3.1950e4$	2.2194	*	$1.4109e4$	8.8047	9.1298	6.2574	26.4898	9.0890
f_3	$1.3027e4$	$3.2368e4$	$6.5316e6$	*	325.5830	361.4643	$4.4152e3$	209.9555	357.5389
f_4	$1.1014e4$	$3.3435e4$	$6.5611e6$	$6.5163e3$	*	0.8389	$4.5597e3$	133.2770	0.8261
f_5	$1.0628e4$	$3.2127e4$	$6.3048e6$	$6.4608e3$	0.4751	*	$4.3802e3$	96.1732	0.0013
f_6	$2.0363e3$	$1.6877e4$	$3.2075e6$	$1.4187e4$	$1.1072e4$	$1.0684e4$	*	$1.0465e4$	$4.0643e3$
f_7	$1.0753e4$	$3.2514e4$	$6.3806e6$	$1.4661e4$	3.3969	2.2095	$4.4334e3$	*	2.2073
f_8	$1.0587e4$	$3.2128e4$	$6.3050e6$	$6.4594e3$	0.4679	0.0013	$4.3803e3$	95.7640	*

is applied to optimize the placement of test points. We set the algorithm population size as 50. The maximum number of iterations is 100, the number of producers is 20% of the population size, the optimization variable dimension is 12, and the optimization objective number is 3. There are few relevant studies on the optimal design of fault diagnosability. Considering that the test point placement approach in Ref. [27] is also based on fault diagnosability evaluation, the proposed approach is compared to that in Ref. [27]. Ref. [27] used NSGA-II to optimize the placement of test points. We set the crossover probability to 0.8 and the mutation probability to 0.1 in NSGA-II. The rest parameters are the same as in this paper. The obtained results are shown in Fig. 5, and the specific results of optimal test point placement are given in Table. 5.

As shown in Fig. 5 and Table 5, if 85% of the maximum system fault diagnosability is the minimum requirement for test point optimal placement, two optimal placement schemes can be obtained using the proposed approach: $\bar{\Omega}_1 = \{t_2, t_6, t_8\}$ and $\bar{\Omega}_2 = \{t_2, t_6, t_9\}$. Two optimal placement schemes can be obtained using the approach in Ref. [27]: $\bar{\Omega}_3 = \{t_2, t_4, t_6, t_9\}$ and $\bar{\Omega}_4 = \{t_2, t_6, t_8, t_{12}\}$. Compared to $\bar{\Omega}_1$ and $\bar{\Omega}_2$, $\bar{\Omega}_3$ and $\bar{\Omega}_4$ require one extra test point for the same diagnosability requirement, resulting in lower reliability and higher cost. All three objectives of $\bar{\Omega}_3$ and $\bar{\Omega}_4$ are inferior to $\bar{\Omega}_1$, $\bar{\Omega}_2$, so $\bar{\Omega}_1$, $\bar{\Omega}_2$ are non-dominated solutions, and $\bar{\Omega}_3$, $\bar{\Omega}_4$ are dominated solutions. The reason is that Ref. [27] performs test point optimal placement based on NSGA-II, which has the problem of not being able to identify pseudo-dominated solutions and easily falling into local

TABLE 5. Results of test point optimal placement.

	Scheme number	Test point set	n	R	C	FDI	FII
The proposed approach	1	$\bar{\Omega}_1 = \{t_2, t_6, t_8\}$	3	0.65	1.60	7.5592	48.1508
	2	$\bar{\Omega}_2 = \{t_2, t_6, t_9\}$	3	0.60	1.65	7.4589	48.7678
Approach in Ref. [27]	3	$\bar{\Omega}_3 = \{t_2, t_4, t_6, t_9\}$	4	0.90	2.45	7.4589	48.7682
	4	$\bar{\Omega}_4 = \{t_2, t_6, t_8, t_{12}\}$	4	1.10	2.20	8.1595	48.1520

TABLE 6. Fault diagnosability evaluation result when t_2, t_6, and t_8 are placed.

	f_0	f_1	f_2	f_3	f_4	f_5	f_6	f_7	f_8
f_1	1.0301	*	0.2341	1.4096	0.8693	0.8510	1.0287	0.8485	0.8511
f_2	1.0301	0.2341	*	1.4073	0.9877	0.9689	1.0287	0.9666	0.9689
f_3	1.4100	1.4096	1.4073	*	1.4096	1.4099	1.4095	1.4080	1.4098
f_4	0.9833	0.8693	0.9877	1.4096	*	0.1844	0.9825	0.1080	0.1846
f_5	0.9852	0.8510	0.9689	1.4099	0.1844	*	0.9847	0.0887	0.0033
f_6	0.1363	1.0287	1.0287	1.4095	0.9825	0.9847	*	0.9984	0.9846
f_7	0.9991	0.8485	0.9666	1.4080	0.1080	0.0887	0.9984	*	0.0890
f_8	0.9851	0.8511	0.9689	1.4098	0.1846	0.0033	0.9846	0.0890	*

TABLE 7. Fault diagnosability evaluation result when t_2, t_6, and t_9 are placed.

|	f_0	f_1	f_2	f_3	f_4	f_5	f_6	f_7	f_8
f_1	1.0227	*	0.2341	1.4096	0.8712	0.8964	1.0214	0.8522	0.8991
f_2	1.0232	0.2341	*	1.4073	0.9897	0.9734	1.0220	0.9702	0.9737
f_3	1.4100	1.4096	1.4073	*	1.4096	1.4099	1.4095	1.4080	1.4098
f_4	0.9482	0.8712	0.9897	1.4096	*	0.2556	0.9474	0.1620	0.2588
f_5	0.9638	0.8964	0.9734	1.4099	0.2556	*	0.9634	0.1345	0.0037
f_6	0.1363	1.0214	1.0220	1.4095	0.9474	0.9634	*	0.9901	0.9636
f_7	0.9907	0.8522	0.9702	1.4080	0.1620	0.1345	0.9901	*	0.1377
f_8	0.9640	0.8991	0.9737	1.4098	0.2588	0.0037	0.9636	0.1377	*
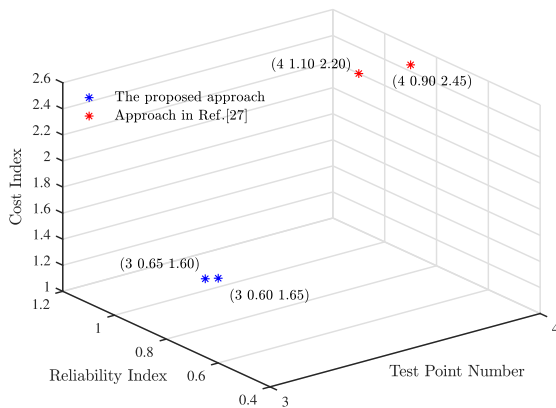
FIGURE 5. Results of the proposed approach and approach in Ref. [27].

optima when solving optimization problems. Therefore, compared with the approach in Ref. [27], the proposed approach requires fewer parameters to be set. The position updates enrich the population diversity after individuals are aware of the danger, reduce the probability of the algorithm falling into local optimum, and improve the global searchability.

$\bar{\Omega}_1$ and $\bar{\Omega}_2$ have the same test points number. Scheme 1 has lower cost and higher fault detectability, and scheme 2 has

better reliability and higher fault isolability. Different schemes can be chosen as the optimal test point placement scheme focusing on different practical requirements. The fault diagnosability quantitative evaluation results corresponding to $\bar{\Omega}_1$ and $\bar{\Omega}_2$ are shown in Table. 6 and Table. 7. We take $\bar{\Omega}_1 = \{t_2, t_6, t_8\}$ as an example. The test signals of each fault at the t_2, t_6, t_8 are shown in Fig. 6. A 1D-CNN model is used to verify the actual fault diagnosis effect when test points t_2, t_6, and t_8 are placed. First, the test signals of t_2, t_6, and t_8 are sampled and combined together, with each sample having a length of 1536. The CNN model consists of an input layer, two convolutional layers, two pooling layers, a fully connected layer, a softmax classifier, and an output layer. The parameters of the CNN are shown in Table 8. Then, the fault diagnosis results under balanced and unbalanced datasets are analyzed, respectively. In the balanced data set, the normal samples and all kinds of fault samples in the training set are 300, and the normal samples and fault samples in the test set are 100. In the unbalanced dataset, the normal samples in the training set are 300, and the fault samples of each type are 60. The ratio of normal samples to fault samples in the test set is unchanged. The distribution of datasets is shown in Table 9.
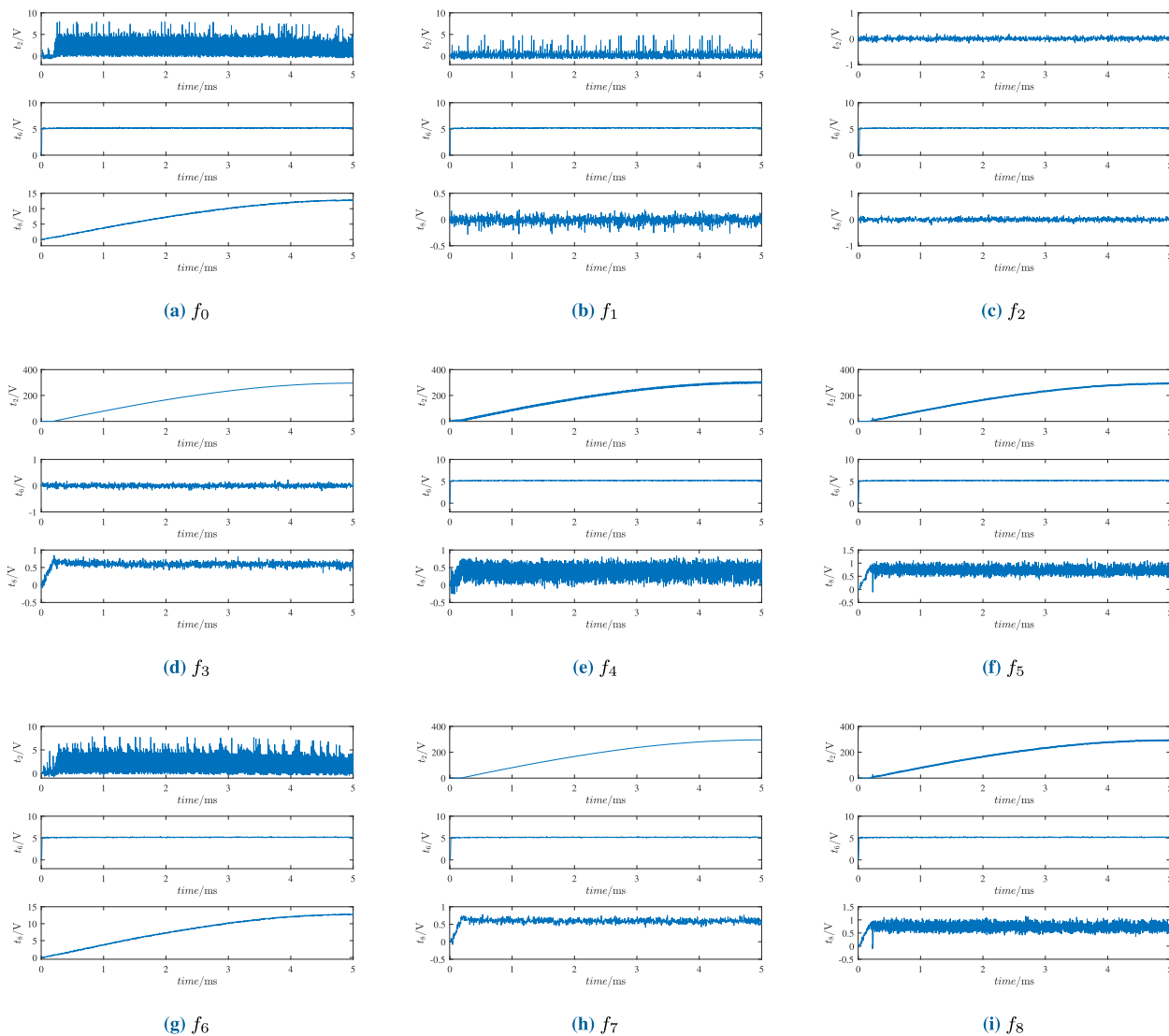
FIGURE 6. Test signal of t_2, t_6 and t_8.

TABLE 8. Parameter of the CNN model.

Layer name	Parameter	Layer size
Input Layer	-	$1 * 1536 * 1$
Convolutional Layer1	Conv(1×6), kernel size=7	$6 * 1530 * 1$
Pooling Layer1	kernel size=5	$6 * 306 * 1$
Convolutional Layer2	Conv(6×9), kernel size=7	$9 * 300 * 1$
Pooling Layer2	kernel size=5	$9 * 60 * 1$
Fully Connected Layer1	-	$540 * 120$
Fully Connected Layer2	-	$120 * 84$
Output Layer	-	$84 * 9$

The labels of faults $f_1 - f_8$ are set to 1-8, respectively, and the label of f_0 is set to 9. Set the learning rate as 0.005, batch size as 16, total epoch as 100, the activation function is RELU, and the loss function is cross entropy. The fault diagnosis results in both cases are given in a confusion matrix, as shown in Fig. 7 and Fig. 8. According to Fig. 7, when there are sufficient fault samples, all the samples of the remaining classes can be correctly classified except f_5, i.e., all faults

TABLE 9. Distribution of the dataset.

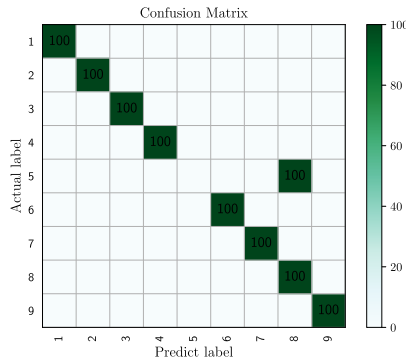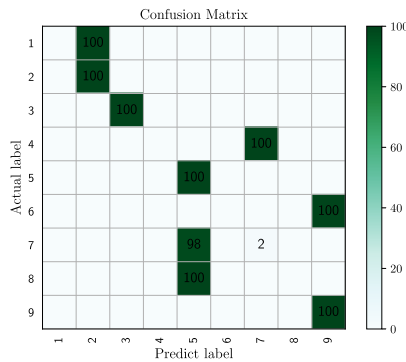|	Unbalanced cases	Size of normal condition		Size of each kind of fault conditions	
		Training dataset	Testing dataset	Training dataset	Testing dataset
Case 1	1:1	300	100	300	100
Case 2	5:1	300	100	60	100

FIGURE 7. Confusion matrix for case 1.

FIGURE 8. Confusion matrix for case 2.

except f_5 can be detected and isolated. All samples of f_5 are classified as f_8, indicating that the samples of f_5 and f_8 cannot be distinguished. Since $D(f_5, f_8) = 0.0033$ in the fault diagnosability evaluation result, f_5 and f_8 are not isolable. The fault diagnosis result is consistent with the conclusion of the fault diagnosability evaluation. According to Fig. 8, when the fault samples are unbalanced, all samples of f_6 are classified as f_0. According to the fault diagnosis results, f_6 cannot be detected, while the other faults can be detected. The fault detectability of f_6 is the lowest, and detecting f_6 is the most difficult. The detectability of the remaining faults is much higher than f_6. Therefore, other faults can still be detected when f_6 cannot be detected. Similarly, it can be found that misclassified faults have lower fault isolability between them: $D(f_1, f_2) = 0.2341$, $D(f_4, f_7) = 0.1080$, $D(f_5, f_8) = 0.0033$, $D(f_5, f_7) = 0.0887$. Therefore, the diagnosability evaluation results can reflect the fault diagnosed capability.

Compared to placing all test points, when only test points t_2, t_6, t_8 are placed, the fault diagnosability quantitative

evaluation indexes of some faults are reduced due to the reduction of measurement information. For example, the fault detectability index of f_6 is reduced from 0.9708 to 0.1363, and the fault isolability index between f_7 and f_8 is reduced from 0.4462 to 0.0890. However, from the perspective of overall system reliability and cost, since only place three test points, the overall system reliability is improved, and the cost is reduced without changing the qualitative properties of fault detectability and isolability. At the same time, the fault diagnosability quantitative indexes achieve the expected requirements to be achieved, which proves the effectiveness of the method proposed in this paper.

V. CONCLUSION

This paper investigates the problem of optimal test point placement based on the fault diagnosability evaluation. The innovations of this paper mainly include the following three points.

1) We consider the influence of test point placement on the ease of fault diagnosis. It incorporates fault diagnosability as a design feature into the system design process, thus fundamentally improving the ability to diagnose faults.

2) A fault diagnosability quantitative evaluation approach based on MMD is proposed. It does not need to construct an analytical model and quantitatively evaluate the fault diagnosability based on measurement data.

3) Considering the test point configuration as a multi objective optimization problem, a multi objective optimization model is designed with the fault diagnosability index as the constraint and the number of test points, reliability index, and cost index as the optimization objectives. The multi objective sparrow search algorithm is used to solve the optimal test points set that satisfy the fault diagnosability index.

REFERENCES

[1] X. Yin, J. Chen, Z. Li, and S. Li, "Robust fault diagnosis of stochastic discrete event systems," *IEEE Trans. Autom. Control*, vol. 64, no. 10, pp. 4237–4244, Oct. 2019.

[2] S. Dey, H. E. Perez, and S. J. Moura, "Robust fault detection of a class of uncertain linear parabolic PDEs," *Automatica*, vol. 107, pp. 502–510, Sep. 2019.

[3] Y. Song, Y. Li, L. Jia, and M. Qiu, "Retraining strategy-based domain adaption network for intelligent fault diagnosis," *IEEE Trans. Ind. Informat.*, vol. 16, no. 9, pp. 6163–6171, Sep. 2020.

[4] *IEEE Trial-Use Standard for Testability and Diagnosability Characteristics and Metrics*, IEEE Standard 1522, 2005.

[5] D. Wang, F. Fu, C. Liu, W. Li, W. Liu, Y. He, and Y. Xing, "Connotation and research status of diagnosability of control systems: A review," *Acta Automat. Sinica*, vol. 44, no. 9, pp. 1537–1553, Sep. 2018.

[6] W. B. Li, D. Y. Wang, and C. R. Liu, "Quantitative fault diagnosis ability evaluation for control systems with disturbances," *Control Theory Appl.*, vol. 32, no. 6, pp. 744–752, Jun. 2015.

[7] W. Liu, W. Li, X. Zhang, and C. Liu, "Fault diagnosability evaluation of deep space exploration spacecraft based on graph theory," *Control Theory Appl.*, vol. 36, no. 12, pp. 2074–2084, Dec. 2019.

[8] J. Liu, Y. Hua, Q. Li, and Z. Ren, "Fault diagnosability qualitative analysis of spacecraft based on temporal fault signature matrix," in *Proc. IEEE Chin. Guid., Navigat. Control Conf.*, Nanjing, China, Aug. 2016, pp. 1496–1500.

[9] F. Fu, D. Wang, L. Li, W. Li, and Z. Wu, "Data-driven method for the quantitative fault diagnosability analysis of dynamic systems," *IET Control Theory Appl.*, vol. 13, no. 8, pp. 1197–1203, Apr. 2019.

[10] F. Fu, T. Xue, Z. Wu, and D. Wang, "A fault diagnosability evaluation method for dynamic systems without distribution knowledge," *IEEE Trans. Cybern.*, vol. 52, no. 6, pp. 5113–5123, Jun. 2022.

[11] F. Fu and D. Wang, "A method for quantitative fault diagnosability analysis of systems with probabilistic sensor faults," *Int. J. Control, Autom. Syst.*, vol. 17, no. 8, pp. 2159–2164, May 2019.

[12] F. Fu, D. Wang, W. Li, and F. Li, "Data-driven fault identifiability analysis for discrete-time dynamic systems," *Int. J. Syst. Sci.*, vol. 51, no. 2, pp. 404–412, Jan. 2020.

[13] D. Jiang, W. Li, J. Wang, and X. Sun, "Research on sensor optimal placement method using quantitative evaluation of fault diagnosability," *Acta Automat. Sinica*, vol. 44, no. 6, pp. 1128–1137, Jun. 2018.

[14] W. Ye, X. Lv, X. Lv, and L. Ma, "Optimized test selection method considering critical faults," *Syst. Eng. Electron.*, vol. 41, no. 7, pp. 1583–1589, Jul. 2019.

[15] H. Sun, B. Jing, Y. Huang, L. Li, and P. Chen, "Optimization of unreliable test points based on artificial immune clone selection algorithm," *J. Electron. Meas. Instrum.*, vol. 35, no. 2, pp. 152–160, Feb. 2021.

[16] L. Han, X. Shi, and Y. Zhai, "Test optimization selection method based on NSGA-3 and improved Bayesian network model," *J. Northwestern Polytech. Univ.*, vol. 39, no. 2, pp. 414–422, Apr. 2021.

[17] S. Saeedi, S. H. Pishgar, and M. Eslami, "Optimum test point selection method for analog fault dictionary techniques," *Anal. Integr. Circuits Signal Process.*, vol. 100, no. 1, pp. 167–179, Jul. 2019.

[18] Y. Zhai, X. Shi, S. Yang, and Y. Qin, "Multi-objective test optimization selection based on NSGA-II under unreliable test conditions," *J. Beijing Univ. Aeronaut. Astronaut.*, vol. 47, no. 4, pp. 792–801, Apr. 2021.

[19] A. A. Yassine, A. Rosich, and S. Ploix, "An optimal sensor placement algorithm taking into account diagnosability specifications," in *Proc. IEEE Int. Conf. Autom., Quality Test., Robot. (AQTR)*, Cluj-Napoca, Romania, May 2010, pp. 1–6, doi: 10.1109/AQTR.2010.5520799.

[20] L. Liu, X. Hu, X. Peng, and B. Wan, "Methods of sensor placement for fault diagnosis," *J. Xiamen Univ., Natural Sci.*, vol. 55, no. 3, pp. 434–440, May 2016.

[21] Q. Song, R. Wang, and M. Xu, "Design of sensor location for fault detection based on fuzzy probabilistic SDG model," *Comput. Meas. Control*, vol. 17, no. 10, pp. 1895–1897, Apr. 2009.

[22] M. Long, J. Wang, G. Ding, S. J. Pan, and P. S. Yu, "Adaptation regularization: A general framework for transfer learning," *IEEE Trans. Knowl. Data Eng.*, vol. 26, no. 5, pp. 1076–1089, May 2014.

[23] X. Jia, M. Zhao, Y. Di, Q. Yang, and J. Lee, "Assessment of data suitability for machine prognosis using maximum mean discrepancy," *IEEE Trans. Ind. Electron.*, vol. 65, no. 7, pp. 5872–5881, Jul. 2018.

[24] X. Li, H. Jiang, R. Wang, and M. Niu, "Rolling bearing fault diagnosis using optimal ensemble deep transfer network," *Knowl.-Based Syst.*, vol. 213, Feb. 2021, Art. no. 106695.

[25] B. Han, X. Zhang, J. Wang, Z. An, S. Jia, and G. Zhang, "Hybrid distance-guided adversarial network for intelligent fault diagnosis under different working conditions," *Measurement*, vol. 176, May 2021, Art. no. 109197.

[26] Y. Wang, D. Wu, and X. Yuan, "LDA-based deep transfer learning for fault diagnosis in industrial chemical processes," *Comput. Chem. Eng.*, vol. 140, Sep. 2020, Art. no. 106964.

[27] D.-N. Jiang and W. Li, "Multi-objective optimal placement of sensors based on quantitative evaluation of fault diagnosability," *IEEE Access*, vol. 7, pp. 117850–117860, 2019.

[28] F. Z. Fu, D. Y. Wang, and W. B. Li, "Quantitative evaluation of actual LOE fault diagnosability for dynamic systems," *Acta Automat. Sinica*, vol. 43, no. 11, pp. 1941–1949, Nov. 2017.

[29] A. Gretton, K. M. Borgwardt, M. J. Rasch, B. Schölkopf, and A. Smola, "A kernel two-sample test," *J. Mach. Learn. Res.*, vol. 13, pp. 723–773, Mar. 2012.

[30] J. Kellner and A. Celisse, "A one-sample test for normality with kernel methods," *Bernoulli*, vol. 25, no. 3, pp. 1816–1837, Aug. 2019.

[31] J. Xue and B. Shen, "A novel swarm intelligence optimization approach: Sparrow search algorithm," *Syst. Sci. Control Eng.*, vol. 8, no. 1, pp. 22–34, Jan. 2020.

[32] W. Tuerxun, X. Chang, G. Hongyu, J. Zhijie, and Z. Huajian, "Fault diagnosis of wind turbines based on a support vector machine optimized by the sparrow search algorithm," *IEEE Access*, vol. 9, pp. 69307–69315, 2021.

XIAN-JUN SHI received the Ph.D. degree in control science and engineering from Naval Aviation University, China, in 2012. He is currently working as a Professor at Naval Aviation University. His research interests include system fault diagnosis, testability modeling, and testability optimization design.

YU-FENG QIN received the B.S. degree in control science and engineering from Harbin Engineering University, Harbin, China, in 2012, and the M.S. degree in control science and engineering from Naval Aviation University, Yantai, China, in 2016, where he is currently pursuing the Ph.D. degree in control science and engineering. His research interests include fault diagnosis and fault diagnosability optimization design.

LI ZHAO received the B.S. degree in control science and engineering from Naval Aviation University, Yantai, China, in 2020, where he is currently pursuing the M.S. degree in control science and engineering. His research interest includes intelligent fault diagnosis.

● ● ●